

Matter-wave solitons in nonlinear optical lattices

Hidetsugu Sakaguchi¹ and Boris A. Malomed²

¹*Department of Applied Science for Electronics and Materials, Interdisciplinary Graduate School of Engineering Sciences, Kyushu University, Kasuga, Fukuoka 816-8580, Japan*

²*Department of Interdisciplinary Studies, School of Electrical Engineering, Faculty of Engineering, Tel Aviv University, Tel Aviv 69978, Israel*

(Received 19 May 2005; revised manuscript received 11 July 2005; published 24 October 2005)

We introduce a dynamical model of a Bose-Einstein condensate based on the one-dimensional (1D) Gross-Pitaevskii equation (GPE) with a nonlinear optical lattice (NOL), which is represented by the cubic term whose coefficient is periodically modulated in the coordinate. The model describes a situation when the atomic scattering length is spatially modulated, via the optically controlled Feshbach resonance, in an optical lattice created by interference of two laser beams. Relatively narrow solitons supported by the NOL are predicted by means of the variational approximation (VA), and an averaging method is applied to broad solitons. A different feature is a minimum norm (number of atoms), $N=N_{\min}$, necessary for the existence of solitons. The VA predicts N_{\min} very accurately. Numerical results are chiefly presented for the NOL with the zero spatial average value of the nonlinearity coefficient. Solitons with values of the amplitude A larger than at $N=N_{\min}$ are stable. Unstable solitons with smaller, but not too small, A rearrange themselves into persistent breathers. For still smaller A , the soliton slowly decays into radiation without forming a breather. Broad solitons with very small A are practically stable, as their decay is extremely slow. These broad solitons may freely move across the lattice, featuring quasielastic collisions. Narrow solitons, which are strongly pinned to the NOL, can easily form stable complexes. Finally, the weakly unstable low-amplitude solitons are stabilized if a cubic term with a constant coefficient, corresponding to weak attraction, is included in the GPE.

DOI: [10.1103/PhysRevE.72.046610](https://doi.org/10.1103/PhysRevE.72.046610)

PACS number(s): 05.45.Yv, 03.75.Lm, 42.65.Tg

I. INTRODUCTION

The possibility to create matter-wave solitons in Bose-Einstein condensates (BECs) has attracted a great deal of attention due to a number of successful experimental results reported in effectively one-dimensional (1D) settings. First, dark solitons were made in repulsive condensates [1], i.e., ones with a positive scattering length that determines the sign of the effective cubic nonlinearity in the corresponding Gross-Pitaevskii equation (GPE). This was followed by the creation of bright solitons in attractive BECs (in lithium) with a negative scattering length [2]. Recently, broad solitons of the gap type (a different species of bright solitons) were created in a repulsive rubidium condensate loaded in an optical lattice (OL), i.e., a spatially periodic atomic potential of the dipole interaction induced by a superposition of counter-propagating coherent laser beams illuminating the condensate, with a frequency appropriately detuned from the internal frequency of atoms [3].

For the experimental and theoretical considerations alike, an important tool is the Feshbach resonance (FR), which makes it possible to control the size of the scattering length and, moreover, switch its sign, by means of external magnetic field [4] (in particular, switching from repulsion to weak attraction was instrumental in the creation of the bright solitons in lithium [2]). Application of ac magnetic field may provide for periodic alternation of the nonlinearity sign in the GPE via the FR. It has been demonstrated theoretically that the ac variety of the FR technique gives rise to interesting states in the 1D geometry [5], and stabilizes two-dimensional (2D) solitons against collapse, even without an external trap [6]. It was also shown that the same

technique may stabilize single- and multihumped 3D matter-wave solitons, provided that it is applied in combination with a quasi-1D OL potential [7].

Some time ago it was predicted [8], and recently demonstrated in an experiment [9], that the FR controlling collisions between atoms and, eventually, the size and sign of the nonlinearity coefficient in the GPE can be induced not only by dc magnetic field, but also by an appropriately tuned optical signal. This suggests a possibility to create a superposition of two coherent beams inducing the optical FR, which will be a *nonlinear optical lattice* (NOL), i.e., a configuration with the local nonlinearity coefficient periodically modulated as a function of the spatial coordinate(s).

Recently, nonlinear photonic lattices have drawn considerable interest in optics, where they were created experimentally and studied theoretically in photorefractive (PhR) media, see a recent review [10] and references therein, and some other recent papers stressing the nonlinear character of photonic lattices in this setting [11]. The lattice in a PhR crystal is created by illuminating it with counterpropagating coherent laser beams in the ordinary polarization (a probe beam that creates solitons is then launched in the extraordinary polarization). A possibility to create a nonlinear lattice this way is very natural, as PhR media feature saturable nonlinearity [10].

Unlike the PhR media, in BECs the self-focusing nonlinearity is strictly cubic (except for the case of a truly one-dimensional Boson gas with very strong ultralocal repulsion, which obeys the GPE with a *quintic* self-defocusing nonlinear term [12]). For this reason, the use of the nonlinearity coefficient spatially modulated by the standing light wave via the optically controlled FR is a unique possibility to cre-

ate a NOL for matter waves in BEC. The objective of this work is to study bright solitons in this setting in the 1D case.

Strictly speaking, the objects that we are going to study are not solitons in the mathematically rigorous meaning, but rather “solitary waves,” as they appear in a nonintegrable model. Nevertheless, the application of the word “soliton” to localized pulses in BECs is commonly adopted in physics literature (see, e.g., Refs. [1–3,6,7,14]), therefore we also use this word in the present paper.

The paper is organized as follows. In Sec. II, the model is formulated, and analytical results for 1D solitons are obtained by means of the variational approximation (VA), which applies to narrow solitons, and by means of the averaging method for the opposite case of very broad solitons. Basic numerical results, for the model with zero average value of the nonlinearity coefficient, are reported in Sec. III. The results show that stability of the solitons strongly depends on their amplitude: while high-amplitude solitons are stable, and low-amplitude ones are not, featuring very slow decay, solitons with intermediate values of the amplitude are more unstable and spontaneously rearrange themselves into robust periodically oscillating breathers. In Sec. IV, additional results are reported. In particular, we demonstrate that the low-amplitude solitons may move freely through the NOL, and collisions between them are quasielastic. On the other hand, high-amplitude solitons, which are strongly pinned by the lattice, can easily form stable bound complexes. It is also shown that the addition of a small nonzero average value of the nonlinearity coefficient which corresponds to self-attraction leads to stabilization of broad small-amplitude solitons. The paper is concluded by Sec. V.

II. MODEL AND ANALYTICAL APPROXIMATIONS

A. Gross-Pitaevskii equation with the nonlinear optical lattice

We start with the effective one-dimensional GPE for the single-atom wave function ψ , written in the well-known normalized form (with \hbar and the atomic mass set equal to 1, see further details in the above-mentioned papers), in which the coefficient in front of the cubic term may be a function of the coordinate x , due to the FR controlled by the standing light wave, as explained above,

$$i\psi_t = -\frac{1}{2}\psi_{xx} + g(x)|\psi|^2\psi. \quad (1)$$

This equation does not include an external trap, as we are interested in stable solitons supported solely by the NOL. The spatial distribution of the optical intensity $I(x)$ in the standing wave with the wavelength λ , which controls the FR, is, as usual, given by

$$I = I_0 \cos^2(2\pi x/\lambda); \quad (2)$$

using the remaining scale invariance in Eq. (1), we set $\lambda \equiv 2\pi$. The dependence of the FR-controlled atomic scattering length [in other words, of the nonlinearity coefficient g in Eq. (1)] on I is [8]

$$g = g_0 + g_1 I / (\delta + I), \quad (3)$$

where g_0 is its value in the absence of the light signal, g_1 is a constant, and δ , which may be either positive or negative, measures the resonance detuning. Thus, assuming a weak optical signal, $I_0 \ll |\delta|$, Eqs. (2) and (3) give rise to the following form of the FR-controlled GPE, in which the coefficient in front of the x -dependent part of the nonlinearity coefficient was set equal to -1 , by rescaling the wave function and shifting x by π , if g_1 was originally positive:

$$i\psi_t = -\frac{1}{2}\psi_{xx} + [g_0 - \cos(2x)]|\psi|^2\psi. \quad (4)$$

Note that the intensity-independent nonlinear coefficient g_0 may be altered independently, by means of the magnetic-controlled FR. Taking this possibility into regard, in a larger part of this work we focus on the case of $g_0=0$, as it corresponds to a completely different situation in comparison with earlier studied models. However, some results will also be given for $g_0 \neq 0$. Equation (4) has two dynamical invariants, viz. the Hamiltonian

$$H = \frac{1}{2} \int_{-\infty}^{+\infty} [|\psi_x|^2 + [g_0 - \cos(2x)]|\psi|^4] dx, \quad (5)$$

and the norm (number of atoms),

$$N = \int_{-\infty}^{+\infty} |\psi(x)|^2 dx. \quad (6)$$

Generally speaking, the NOL may come together with its linear counterpart, i.e., a term proportional to $\cos(2x)\psi$ in Eq. (4). However, this term may be neglected if the light wavelength necessary for the optically induced FR which affects the interaction between atoms (usually, it corresponds to blue light) is far from the wavelength (usually, corresponding to mid-infrared) which induces the linear OL potential for a single atom.

B. Variational approximation

Stationary solutions to Eq. (4) are sought for as $\psi(t, x) = e^{-i\mu t} \phi(x)$, with the real function ϕ obeying the equation

$$\mu\phi + \frac{1}{2} \frac{d^2\phi}{dx^2} - [g_0 - \cos(2x)]\phi^3 = 0. \quad (7)$$

To apply the variational approximation (VA), we rely upon the fact that the stationary equation (7) can be derived from the Lagrangian

$$L = \int_{-\infty}^{+\infty} \left[2\mu\phi^2 - \left(\frac{d\phi}{dx} \right)^2 + [\cos(2x) - g_0]\phi^4 \right] dx. \quad (8)$$

The variational ansatz for the soliton is adopted in the usual Gaussian form,

$$\phi(x) = A \exp\left(-\frac{x^2}{2W^2}\right), \quad (9)$$

with the amplitude A and width W . The substitution of the ansatz in Eq. (8) yields an effective Lagrangian,

$$\begin{aligned} L_{\text{eff}} &= 2\sqrt{\pi}\mu A^2 W - \frac{\sqrt{\pi}A^2}{2} W \\ &- \sqrt{\frac{\pi}{2}}g_0 A^4 W + \sqrt{\frac{\pi}{2}}A^4 W \exp\left(-\frac{W^2}{2}\right) \\ &= 2\mu N - \frac{N}{2W^2} - \frac{g_0 N^2}{\sqrt{2\pi}W} + \frac{N^2}{\sqrt{2\pi}W} \exp\left(-\frac{W^2}{2}\right), \end{aligned} \quad (10)$$

where the amplitude was eliminated in favor of the norm of ansatz (9), which is defined as per Eq. (6),

$$N = \sqrt{\pi}A^2 W. \quad (11)$$

The variational equations, $\partial L_{\text{eff}}/\partial N = \partial L_{\text{eff}}/\partial W = 0$, yield a system

$$N = \frac{\sqrt{2\pi}}{W[(1+W^2)e^{-W^2/2} - g_0]}, \quad (12)$$

$$\mu = -\frac{3g_0 + (W^2 - 3)e^{-W^2/2}}{[3g_0 - 4(1+W^2)e^{-W^2/2}]W^2}. \quad (13)$$

The first prediction of Eq. (12) is that there is no physical solution in the case when the constant nonlinearity coefficient corresponds to strong self-repulsion, $g_0 \geq 2/\sqrt{e} \approx 1.21$. For $0 \leq g_0 < 2/\sqrt{e}$, Eq. (12) predicts a family of solitons in the interval $N_{\min} < N < \infty$, where

$$N_{\min} = \frac{\sqrt{2\pi}}{W_0[(1+W_0^2)e^{-W_0^2/2} - g_0]}, \quad (14)$$

W_0 being a positive root of the transcendental equation

$$(1 + 2W_0^2 - W_0^4)\exp(-W_0^2/2) = g_0. \quad (15)$$

In fact, direct consideration of Eq. (7) shows that a soliton solution may exist only in the case when the nonlinearity coefficient, $g_0 - \cos(2x)$, is negative at least at the point of a local maximum of $|\phi(x)|$. Indeed, the localized solution may only exist if $\mu < 0$, and the curvature of the wave's profile is negative at the maximum point, hence if $g_0 - \cos(2x)$ is positive at this point, all the terms on the left-hand side of Eq. (7) have the same sign, and the equation cannot hold. Thus it is very natural to assume that solitons exist if $g_0 < 1$, which allows the expression $g_0 - \cos(2x)$ to be negative in some regions. The fact that VA predicts the maximum value of g_0 to be 1.21, i.e., larger than 1, is an error introduced by the approximation (although the error is not large). For this reason, we continue the analysis of the VA for $g_0 < 1$.

A consequence of Eq. (12) is that the width of the soliton takes values $W < W_{\max}$, where W_{\max} is a root of the equation

$$(1 + W_{\max}^2)\exp(-W_{\max}^2/2) = g_0 \quad (16)$$

[from comparison with Eq. (15), it is obvious that $W_0 < W_{\max}$]. Further consideration of Eq. (12) demonstrates that each value of norm N exceeding N_{\min} gives rise to two different solutions with different widths, which belong to the intervals, respectively, $W < W_0$ and $W_0 < W < W_{\max}$. It is natural to expect that the solutions may be stable in the former interval, which is characterized by $dW/dN < 0$ ("heavier" solitons are narrower), and must be unstable in the latter one, which features the inverse dependence, with $dW/dN > 0$. Below, direct numerical simulations will confirm this expectation. The stability change for the soliton solutions at $W = W_0$ is also confirmed by the well-known Vakhitov-Kolokolov (VK) criterion [13]: the transition from $W < W_0$ to $W > W_0$ entails a change from $d\mu/dN < 0$ to $d\mu/dN > 0$, which implies the transition from stable solutions to unstable ones, according to the criterion.

For $g_0 = 0$ (the basic case to be studied in detail below by numerical methods), Eqs. (15) and (16) yield $W_0^2 = 1 + \sqrt{2}$ and $W_{\max} = \infty$ (in fact, the VA is irrelevant for large W , see below). Accordingly, Eq. (14) produces a prediction for the minimum value of the norm necessary for the existence of solitons,

$$N_{\min}(g_0 = 0) = \sqrt{\pi}(\sqrt{2} - 1)^{3/2}e^{(1+\sqrt{2})/2} \approx 1.580. \quad (17)$$

In conclusion, we note that for $g_0 < 0$, when the nonlinear interaction is, on average, self-attractive, the VA yields completely different results: as seen from Eq. (12), there is no lower limit N_{\min} in this case, as $W \rightarrow \infty$ corresponds to $N \rightarrow 0$. Further, if negative g_0 belongs to the interval $0 < -g_0 < 4(2 + \sqrt{6})\exp[-(3 + \sqrt{2})/2] \approx 1.96$, Eq. (15) with $g_0 < 0$ yields two roots, $(W_0)_{\min}$ and $(W_0)_{\max}$. According to the above criteria, the solutions are stable in the regions $0 < W < (W_0)_{\min}$ and $(W_0)_{\max} < W < \infty$, and unstable in between, at $(W_0)_{\min} < W < (W_0)_{\max}$. The former stability region is similar to that found above for $g_0 \geq 0$, while the latter one is specific to negative g_0 . In particular, for $0 < -g_0 \leq 1$, the additional stability region is

$$W_{\max} \approx 2 \ln(1/|g_0|) < W < \infty. \quad (18)$$

For $-g_0 > 4(2 + \sqrt{6})\exp[-(3 + \sqrt{2})/2] \approx 1.96$, the intermediate region does not exist, and all the solitons are expected to be stable, being essentially similar to the usual solitons in the one-dimensional GPE with a constant coefficient of the self-attraction.

C. An approximation for broad solitons

The VA based on the simple Gaussian ansatz (9) is relevant as long as the width W does not essentially exceed the period of the underlying NOL, which is π , in the notation adopted above. If W is larger, the undulated shape of the soliton, induced by the nonlinear OL, cannot be disregarded, see examples below in Figs. 6 and 7. Indeed, even if the amplitude of the undulations is relatively small, which is the case in those figures, its contribution to the Lagrangian term accounting for the nonlinearity [the last term in expression (8)] is crucially important for $g_0 = 0$, as, disregarding the un-

dulations in the soliton's shape, this term, which is the integral convolution of a slowly varying function $\phi^A(x)$ and rapidly oscillating one, $\cos(2x)$, will be exponentially small. In particular, the above-mentioned value $W_0(g_0=0)=\sqrt{1+\sqrt{2}}\approx 1.554$ definitely satisfies the condition $W_0<\pi$, therefore the prediction (17) for the minimum norm of the soliton in the case of $g_0=0$ is a meaningful one.

In the opposite case of very broad solitons, $W\gg\pi$, it is natural to apply the averaging method, searching for a solution in the form of

$$\psi(x,t)=\psi^{(0)}(x,t)+\psi^{(1)}(x,t)\cos(2x)+\dots, \quad (19)$$

where $\psi^{(0)}$ and $\psi^{(1)}$ are slowly varying functions of x (and t), in comparison with the rapidly oscillating function $\cos(2x)$. The substitution of expansion (19) in Eq. (4) yields, first, a relation

$$\psi^{(1)}=\frac{1}{2}|\psi^{(0)}|^2\psi^{(0)}. \quad (20)$$

Further, substituting relations (19) and (20) in Eq. (4) and collecting slowly varying terms, the resulting equation for ψ_0 takes a simple form for $g_0=0$:

$$i\psi_t^{(0)}=-\frac{1}{2}\psi_{xx}^{(0)}-\frac{3}{4}|\psi^{(0)}|^4\psi^{(0)}, \quad (21)$$

which is a *quintic* GPE. A family of exact soliton solutions to Eq. (21) can be easily found for negative values of the chemical potential μ ,

$$\psi_{\text{sol}}(x,t)=e^{-i\mu t}(-\mu)^{1/4}\sqrt{2}\operatorname{sech}(2\sqrt{-\mu}x). \quad (22)$$

The norm of this solution does not depend on μ ,

$$N_{\text{sol}}\equiv\pi. \quad (23)$$

The fact that $dN_{\text{sol}}/d\mu\equiv 0$ implies neutral VK stability. Actually, Eq. (21) with the self-attracting quintic nonlinearity gives rise to *weak collapse* in the one-dimensional setting [15]. Because of the possibility of the collapse, soliton solutions (22), being neutrally stable against exponentially growing perturbations, are unstable against slowly growing (sub-exponential) perturbations.

If small average nonlinearity, corresponding to the term with $g_0\neq 0$ in Eq. (4), is retained in the model, the above averaging procedure leads to an effective *cubic-quintic* (CQ) equation:

$$i\psi_t^{(0)}=-\frac{1}{2}\psi_{xx}^{(0)}+g_0|\psi^{(0)}|^2\psi^{(0)}-\frac{3}{4}|\psi^{(0)}|^4\psi^{(0)}. \quad (24)$$

If the average nonlinearity is attractive, $g_0<0$, the quintic term in Eq. (24) may be neglected, which gives rise to the usual stable nonlinear-Schrödinger solitons for $\mu<0$,

$$\psi(x,t)=\sqrt{\frac{2\mu}{g_0}}e^{-i\mu t}\operatorname{sech}(\sqrt{-2\mu}x). \quad (25)$$

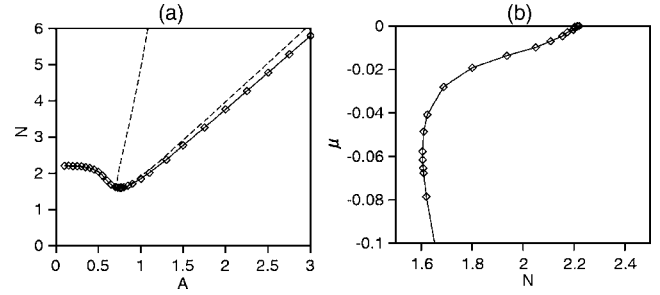


FIG. 1. (a) The norm of the stationary soliton solution to Eq. (7) vs its amplitude, for $g_0=0$. Rhombuses (connected by the continuous line as a guide to the eye) are values found from the direct numerical solution, and the dashed curve shows the prediction of the variational approximation. The branch of the latter solution to the left of $N=N_{\text{min}}$ is an irrelevant one (it corresponds to broad solitons for which the variational approximation is irrelevant, as explained in the text). (b) The chemical potential vs the number of atoms for the numerically found soliton solutions.

In the case of $g_0>0$ (repulsive average nonlinearity), exact soliton solutions to Eq. (24) can be easily found too (actually, they are an analytical continuation of the well-known solutions of the CQ equation with opposite signs in front of the nonlinear terms [16]),

$$\psi_{\text{sol}}(x,t)=2e^{-i\mu t}\sqrt{\frac{-\mu}{\sqrt{g_0^2-4\mu\cosh(\sqrt{-2\mu}x)}-g_0}}, \quad (26)$$

where μ must again be negative. Note that the amplitude A of this solution is limited from below,

$$A^2=\sqrt{g_0^2-4\mu}+g_0\geq 2g_0. \quad (27)$$

The norm of the soliton (26) is

$$N_{\text{sol}}=\sqrt{2}\left[\pi+2\tan^{-1}\left(\frac{g_0}{\sqrt{-2\mu}}\right)\right] \quad (28)$$

(observe that the norm of the soliton family is limited from below and from above, $\sqrt{2}\pi<N_{\text{sol}}<2\sqrt{2}\pi$). It follows from Eq. (28) that $dN_{\text{sol}}/d\mu>0$, hence all these solitons, unlike solution (25), are *unstable*, as per the VK criterion.

III. BASIC NUMERICAL RESULTS

In this section, we focus on the case of $g_0=0$, which is essentially different in comparison with previously studied 1D versions of the GPE. First of all, the stationary equation (7) was solved in a numerical form. That is, the solutions to the second-order differential equation which approach 0 for $|x|\rightarrow\infty$ were numerically searched for various values of $\phi(0)=A$ by changing the value of μ . The results are summarized in Fig. 1, which shows the norm of the soliton vs its amplitude, together with the same dependence as predicted by the VA in an implicit form, based on Eqs. (11) and (12) with $g_0=0$. Examples of the numerically found narrow and broad solitons, along with their approximations based, respectively, on the VA and averaging method, are shown in Fig. 2.

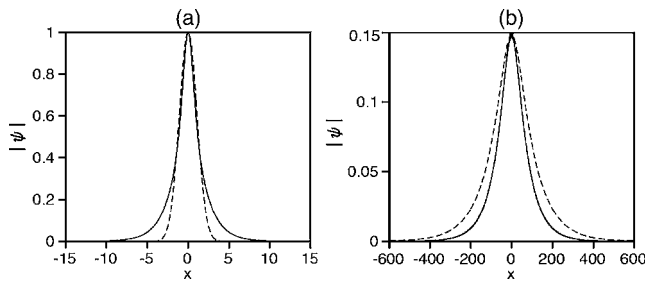


FIG. 2. (a) A typical example of a stable soliton corresponding to $A=1$. The numerically found soliton profile and its counterpart predicted by the variational approximation based on the Gaussian ansatz (9) are shown by the solid and dashed curves, respectively. (b) A typical example of a broad soliton (solid line) corresponding to $A=0.15$ and the approximation (dashed line) based on the averaging method.

Quite a noteworthy feature evident in Fig. 1 is that the VA predicts the minimum norm very accurately, see Eq. (17) [according to the VA, this value is attained at $A=(\sqrt{2}-1)e^{(1+\sqrt{2})/4} \approx 0.757$, which is also fairly accurate, in comparison with the numerical results in 1], and becomes irrelevant [formally predicting a large width, for which ansatz (9) does not apply] almost *immediately* after that point.

The VK criterion, implemented for both the numerically found soliton family [see Fig. 1(b)] and its VA-predicted counterpart, forecasts the solution branch to be stable to the right of the point $N=N_{\min}$ and unstable to the left of it. Consideration of the soliton's width W as a function of N predicts the same result in a different form, less mathematically rigorous but more physically intuitive one. Indeed, the right and left branches have, respectively, $dW/dN < 0$ and $dW/dN > 0$, and, as was already mentioned above, a stable soliton family is expected to satisfy the former condition, while solitons whose width increases with the norm are unlikely to be stable. These nonrigorous but intuitive conditions may also be formulated in terms of the $N(A)$ dependence: solitons are stable if the norm increases with the amplitude, and unstable in the opposite case (recall that the VA-predicted branch to the left of $N=N_{\min}$ is irrelevant, even if it shows $dN/dA > 0$). The stability conditions in the latter form (which are fully corroborated by numerical results) are convenient, as they make it possible to read off the stability of the solitons directly from Fig. 1 for $g_0=0$, or counterparts of this plot for $g_0 \neq 0$ (see Fig. 9 below).

Simulations of evolution of the stationary solitons, with small random initial perturbations explicitly added to them, for the sake of the stability test, completely confirm the above expectations about the stability and instability of the two parts of the soliton family. In particular, the unstable solitons with the initial amplitude from the interval $0.4 < A(0) < 0.75$ spontaneously transform into apparently stable breathers, as shown in Fig. 3. This observation is notable, as the the instability of the solitons to the left of $N=N_{\min}$ in Fig. 1 was predicted by the VK criterion, that captures only instabilities accounted for by eigenmodes of small perturbations with a real instability growth rate, i.e., such an instability cannot immediately transform an unstable soliton into an oscillatory state, unlike the case of instability

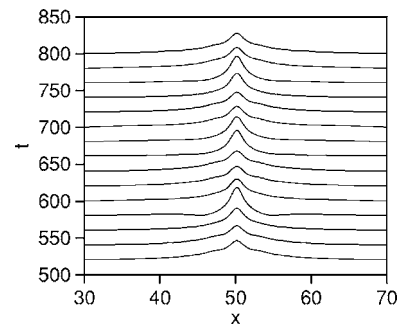


FIG. 3. A typical example of a persistent breather, into which an initial unstable soliton with the amplitude $A=0.6$ has developed, is shown by means of plots of $|\psi(x,t)|$ vs x and t .

against perturbations with complex eigenvalues. In fact, a short initial stage of the evolution is indeed characterized by monotonous growth of the perturbation, which, however, quickly switches into large-amplitude oscillations, see an example [corresponding to $A(0)=0.5$] in Fig. 4.

Solitons with the initial amplitudes from the interval $0.3 < A(0) < 0.4$ are unstable too, but they do not form breathers. Instead, they suffer systematic but slow decay into radiation, gradually decreasing the amplitude and getting broader, as can be seen [for $A(0)=0.35$] in Fig. 4. This conclusion is also confirmed by the plot showing the amplitude of internal oscillations of the breather vs $A(0)$, in Fig. 5 (together with the breather's time-average amplitude): the oscillation amplitude vanishes at $A(0) \approx 0.4$. It is relevant to stress that the amplitude of the oscillations displayed in this figure does not depend on the particular form of small perturbations added to the unstable soliton at the initial moment. Of course, characteristics of the established breather will be different if the onset of instability is initiated by a nonsmall (large-amplitude) perturbation.

For $A(0) < 0.3$, the initial soliton stays practically stable, as can be seen in Fig. 4, where an example is displayed for $A(0)=0.2$. We assume that, strictly speaking, broad solitons from this region are unstable too, but the instability is extremely weak. This conjecture is supported by the fact that, although the soliton family in this region has a positive slope dW/dN —which, as conjectured above, implies the instability—the slope is actually very small [see Fig. 1, where the curve $N(A)$ is almost horizontal for $A \leq 0.3$]. Note

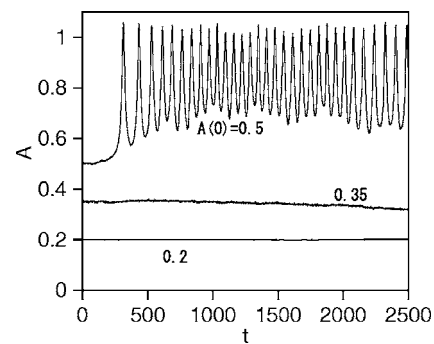


FIG. 4. The evolution of the amplitude of unstable solitons for different values of the initial amplitude $A(0)$.

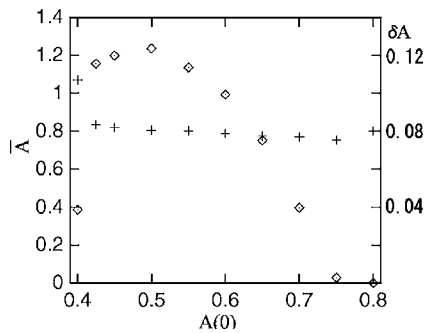


FIG. 5. The amplitude δA of oscillations of the breather (shown by \diamond), together with the breather's amplitude \bar{A} averaged in time (shown by $+$), vs the initial amplitude of the unstable soliton. Note that, as long as the breather is different from a stable stationary soliton, the time-average amplitude is larger than the initial one.

that both the nearly constant value of N for the broad solitons in the region of $A(0) < 0.3$ and their weak instability can be readily explained by the analytical approximation for broad solitons, developed above in the form of Eq. (21). Indeed, the family of soliton solutions to Eq. (21) has a constant norm, as per Eq. (23), although the numerically obtained constant 2.2 of the norm is rather smaller than the theoretical estimate π . As was explained above, these solitons are characterized by weak subexponential instability.

IV. ADDITIONAL RESULTS

The basic results reported above suggest consideration of additional issues. In particular, a natural question is whether a soliton can move without loss across the underlying lattice. As is known, in the case of linear OLs, the soliton becomes mobile below a certain threshold, where the soliton's amplitude is sufficiently small and, accordingly, its width is large enough [14]. A similar effect is observed in the present model including the NOL: the almost-stable broad solitons with $A(0) < 0.3$ can be readily set in motion, and propagates indefinitely long without any conspicuous loss, as illustrated by Fig. 6 for $A(0)=0.25$. No clearly defined maximum velocity is revealed by the simulations, i.e., the soliton can be accelerated, by means of initially multiplying it by $\exp(iKx)$, with a sufficiently large real K , to virtually any value of the velocity.

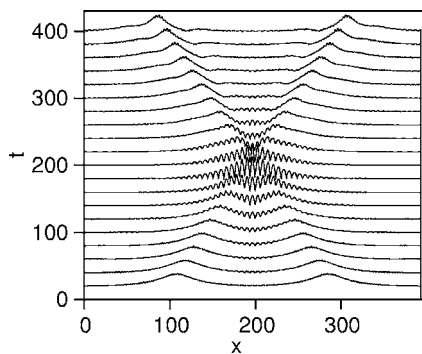


FIG. 7. An example of an elastic collision between two moving broad solitons, with the amplitude $A=0.25$.

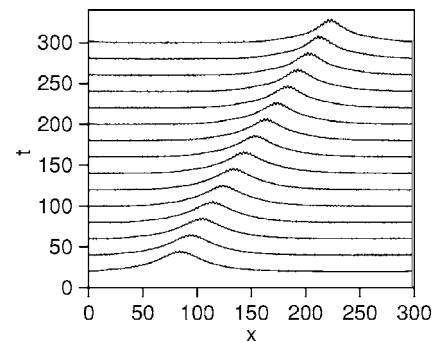


FIG. 6. A freely moving soliton, displayed by means of plots of $|\psi(x,t)|$, with the amplitude $A=0.25$.

The availability of the broad moving solitons makes it possible to consider collisions between them. The result is that collisions are quasielastic, as shown in Fig. 7 (motion of solitons in a model including the cubic nonlinearity and a linear model was recently studied in Ref. [17]). In particular, no visible radiation loss produced by the collisions could be detected. The collisions produces a small shift of the colliding solitons, but this effect is weak and does not seem a physically significant one, in the present context.

On the contrary to the above results, both the absolutely stable narrow solitons with $A > 0.75$, and breathers generated by unstable solitons with $0.4 < A(0) < 0.75$ cannot be made moving, i.e., solitons and breathers with a sufficiently large amplitude are firmly pinned by the nonlinear lattice. An attempt to shove a narrow soliton, multiplying it by $\exp(iKx)$, leads to strongly perturbed and still pinned soliton if K is smaller than a certain critical value K_{cr} . If $K > K_{cr}$, the shove completely destroys the soliton. Examples characterizing this property of the narrow solitons are displayed in Fig. 8.

The strong pinning of narrow solitons facilitates creation of complexes including several of them. Figure 9 displays two examples of stable bound states of two and three solitons, with the phase shift of $\delta = \pi$ between adjacent ones. A bound state of two or three in-phase solitons, with $\delta=0$, can also be found, but it is unstable. We note that, in the case of linear lattices, a general principle states that bound complexes may only be stable with $\delta = \pi$, and they are always unstable for $\delta=0$ [18]. The key point in the proof of this

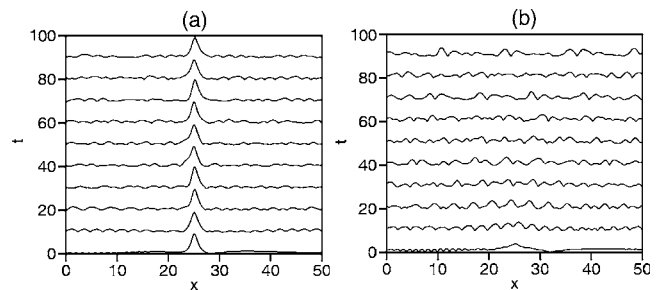


FIG. 8. The result of the attempt to "shove" a narrow stable soliton with the amplitude $A=2$, multiplying it by $\exp(iKx)$: (a) $K=1$; (b) $K=1.7$. In this case, the critical value of the shove strength that leads to complete destruction of the soliton, is $K_{cr} \approx 1.65$.

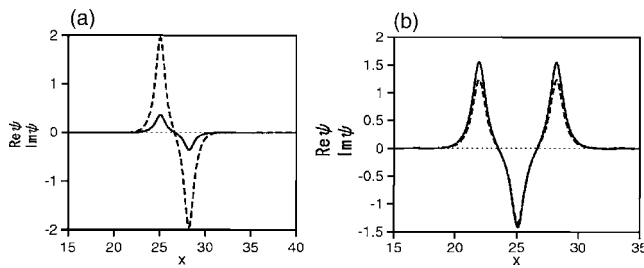


FIG. 9. (a) A stable bound state of two antiphase solitons with the amplitude $A=2$. (b) A stable bound state of three antiphase solitons with the amplitude $A=2$. The solid and dashed lines show, respectively, $\text{Re } \psi(x)$ and $\text{Im } \psi(x)$.

principle is the fact that adjacent solitons with $\delta=\pi$ repel each other; as this feature remains true in the present case (it does not depend on the character of the lattice), it is quite natural that the same necessary condition, $\delta=\pi$, distinguishes stable soliton complexes in the NOL. It is also relevant to mention that stable multisoliton complexes were recently investigated in a model combining a saturable nonlinearity and linear lattice [19].

Last, the general model, which is based on GPE (4) including the term with $g_0 \neq 0$, was investigated too. For small negative g_0 , the basic plot showing N vs A is modified (against the case of $g_0=0$, displayed above in Fig. 1) as shown in Fig. 10(a). An evident implication of the modified $N(A)$ dependence is that small-amplitude large-width solitons, corresponding to the newly appearing segment of the plot with $dN/dA > 0$ [the region $A < 0.4$ in Fig. 10(a)], are *stable* (the soliton family whose norm grows with the amplitude is expected to be stable, as per the above discussion). The stability of these solitons was confirmed by direct simulations, and also by the VK criterion—see Fig. 10(b), where the new branch of the stable solitons corresponds to the top

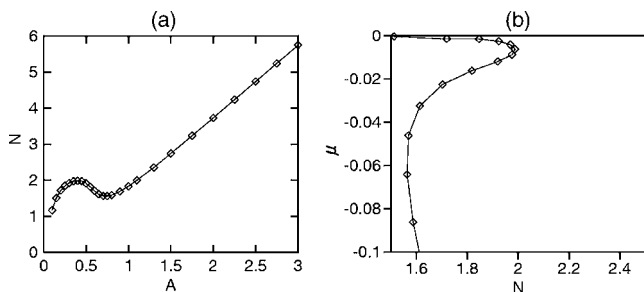


FIG. 10. (a) The norm of the stationary soliton solutions of Eq. (7) vs the amplitude, for $g_0=-0.02$ (cf. Fig. 1 for $g_0=0$). (b) The corresponding $\mu(N)$ dependence, cf. Fig. 1.

part of the curve, with $d\mu/dN < 0$. It is relevant to mention that the VA developed above correctly predicts the emergence of the extra stability region of broad solitons at small negative g_0 , see Eq. (18).

V. CONCLUSION

In this work, we have introduced a 1D model based on the Gross-Pitaevskii equation (GPE) which includes a nonlinear optical lattice (NOL), i.e., the nonlinear term with the coefficient in front of it periodically modulated in the spatial coordinate. The model describes a Bose-Einstein condensate (BEC) in which the scattering length is spatially modulated, through the optically controlled Feshbach resonance, by the optical lattice created by interference of two counterpropagating coherent laser beams.

The existence and stability of relatively narrow solitons supported by the NOL were predicted by means of the variational approximation (VA), and for broad solitons the prediction was based on the averaging method. A different feature in models based on the GPE in one dimension is the existence of a minimum norm (number of atoms), $N=N_{\min}$, necessary for the existence of solitons, in the case when the average nonlinearity coefficient g_0 is zero or positive, corresponding to self-repulsion. The VA predicts this threshold value quite accurately.

Numerical results were presented, chiefly, for the model with $g_0=0$. Solitons with the amplitude exceeding its value at $N=N_{\min}$ are stable (as predicted by the VA), while unstable solitons with smaller, but not very small, amplitudes spontaneously transform themselves into persistent breathers. For a still smaller initial amplitude of the soliton, a breather is not formed, and the soliton slowly decays into radiation. For very small soliton amplitudes, the decay is extremely slow, making the soliton a practically stable object. In the latter case, the solitons may freely move across the NOL, collisions between them being quasielastic. On the other hand, stable narrow solitons, which are strongly pinned to the nonlinear lattice, can easily form stable complexes (at attempt to set narrow solitons in motion strongly perturbs them, and eventually leads to their destruction, but does not create moving objects). The VA very accurately predicts the stable solitons with $N \geq N_{\min}$, and becomes irrelevant past the point of $N=N_{\min}$, as in that case the approximation assumes a broad Gaussian ansatz, which is irrelevant in the present setting. The addition of small $g_0 < 0$ (weak attraction on the average) leads to stabilization of the aforementioned weakly unstable solitons with small amplitudes.

The model can be extended to other physically interesting situations, especially the two-dimensional one. Results for that case will be reported elsewhere.

[1] S. Burger, K. Bongs, S. Dettmer, W. Ertmer, K. Sengstock, A. Sanpera, G. V. Shlyapnikov, and M. Lewenstein, Phys. Rev. Lett. **83**, 5198 (1999); J. Denschlag, J. E. Simsarian, D. L. Feder, C. W. Clark, L. A. Collins, J. Cubizolles, L. Deng, E. W. Hagley, K. Helmerson, W. P. Reinhardt, S. L. Rolston, B. I.

Schneider, and W. D. Phillips, Science **287**, 97 (2000).

[2] L. Khaykovich, F. Scherck, G. Ferrari, T. Bourdel, J. Cubizolles, L. D. Carr, Y. Castin, and C. Salomon, Science **296**, 1290 (2002), K. E. Strecker, G. B. Partridge, A. G. Truscott, and R. G. Hulet, Nature (London) **417**, 153 (2002).

- [3] B. Eiermann, Th. Anker, M. Albiez, M. Taglieber, P. Treutlein, K.-P. Marzlin, and M. K. Oberthaler, *Phys. Rev. Lett.* **92**, 230401 (2004).
- [4] S. Inouye, M. R. Andrews, J. Stenger, H.-J. Miesner, D. M. Stamper-Kurn, and W. Ketterle, *Nature (London)* **392**, 151 (1998); E. A. Donley, N. R. Claussen, S. L. Cornish, J. L. Roberts, E. A. Cornell, and C. E. Wieman, *ibid.* **412**, 295 (2001); H. Saito and M. Ueda, *Phys. Rev. A* **65**, 033624 (2002).
- [5] P. G. Kevrekidis, G. Theocharis, D. J. Frantzeskakis, and B. A. Malomed, *Phys. Rev. Lett.* **90**, 230401 (2003).
- [6] H. Saito and M. Ueda, *Phys. Rev. Lett.* **90**, 040403 (2003); F. Kh. Abdullaev, J. G. Caputo, R. A. Kraenkel, and B. A. Malomed, *Phys. Rev. A* **67**, 013605 (2003); G. D. Montesinos, V. M. Pérez-García, and P. J. Torres, *Physica D* **191**, 193 (2004).
- [7] M. Trippenbach, M. Matuszewski, and B. A. Malomed, *Europhys. Lett.* **70**, 8 (2005); M. Matuszewski, E. Infeld, B. A. Malomed, and M. Trippenbach, *Phys. Rev. Lett.* (to be published).
- [8] P. O. Fedichev, Yu. Kagan, G. V. Shlyapnikov, and J. T. M. Walraven, *Phys. Rev. Lett.* **77**, 2913 (1996).
- [9] M. Theis, G. Thalhammer, K. Winkler, M. Hellwig, G. Ruff, R. Grimm, and J. H. Denschlag, *Phys. Rev. Lett.* **93**, 123001 (2004).
- [10] J. W. Fleischer, G. Bartal, O. Cohen, T. Schwartz, O. Manela, B. Freedman, M. Segev, H. Buljan, and N. K. Efremidis, *Opt. Express* **13**, 1780 (2005).
- [11] D. Neshev, Y. S. Kivshar, H. Martin, and Z. G. Chen, *Opt. Lett.* **29**, 486 (2004); A. S. Desyatnikov, D. N. Neshev, Y. S. Kivshar, N. Sagemerten, D. Trager, J. Jagers, C. Denz, and Y. V. Kartashov, *ibid.* **30**, 869 (2005).
- [12] E. B. Kolomeisky, T. J. Newman, J. P. Straley, and X. Qi, *Phys. Rev. Lett.* **85**, 1146 (2000).
- [13] M. G. Vakhitov and A. A. Kolokolov, *Izv. Vyssh. Uchebn. Zaved., Radiofiz.* **16**, 1020 (1973) [*Radiophys. Quantum Electron.* **16**, 783 (1973)].
- [14] H. Sakaguchi and B. A. Malomed, *J. Phys. B* **37**, 1443 (2004).
- [15] L. Bergé, *Phys. Rep.* **303**, 260 (1998).
- [16] Kh. I. Pushkarov, D. I. Pushkarov, and I. V. Tomov, *Opt. Quantum Electron.* **11**, 471 (1979); S. Cowan, R. H. Enns, S. S. Rangnekar, and S. S. Sanghera, *Can. J. Phys.* **64**, 311 (1986).
- [17] Y. V. Kartashov, A. S. Zelenina, L. Torner, and V. A. Vysloukh, *Opt. Lett.* **29**, 766 (2004).
- [18] T. Kapitula, P. G. Kevrekidis, and B. A. Malomed, *Phys. Rev. E* **63**, 036604 (2001).
- [19] Y. V. Kartashov, V. A. Vysloukh, and L. Torner, *Opt. Express* **12**, 2831 (2004).